

The application of the etch-pit method to quantitative texture analysis

K. T. LEE, G. deWIT, A. MORAWIEC, J. A. SZPUNAR

Department of Metallurgical Engineering, McGill University 3450 University Street, Montreal, Quebec, Canada, H3A 2A7

The etch-pit method is a useful technique for studying the grain orientation in polycrystalline materials. In this paper, the etch-pit method is extended to obtain a quantitative analysis of the texture of materials. From the experimental results, the orientation distribution function (ODF) and the misorientation distribution function (MODF) can be calculated. The computer program developed for this analysis returns the grain size distribution of different texture components and the frequency of coincidence site lattice (CSL) boundaries, as well as other data. This information is used to analyse the grain growth and texture development in transformer steel.

1. Introduction

Understanding the texture development during grain growth requires information about growth behaviour of grains having different orientations. For this purpose, the grain size distribution and the grain orientation are used to complement the orientation distribution function (ODF) which is typically obtained from X-ray diffraction measurements. One method of analysing the grain orientation is the etch-pit method [1–3]. Earlier work [4, 5] had already produced a mathematical procedure for calculating the orientation from certain etch-pits, but the method was not completely understood until L. Yang *et al.* worked on it [6, 7]. Although there has been much research done using this method, most of it has been concerned with the mathematical description of the relationship between the grain orientation and the etch figures. Only recently has the work been done to apply this method to the study of grain orientation distribution and texture [8–10]. In this research a significant number of grains were analysed and classified, grouping their grain orientations and obtaining grain size distributions.

In this paper, a more quantitative technique of data analysis will be introduced. From it, the ODF, the pole figures, the misorientation between neighbouring grains, the frequency of coincidence site lattice (CSL) boundaries, the grain size distribution of certain texture components and other useful information are obtained by digitizing the shape of etch-pits and the grain boundaries.

2. Experimental procedure

To determine the grain orientation, etch-pits were obtained using various chemical etchants. As an example, the etching procedure for silicon steel is itemized in Table I. Statistical analysis of the experimental results reveals the characteristics of the grain

TABLE I Etching procedure for silicon steel

	Solution	Immersion time
Step 1	5%HF + 95% H ₂ O ₂	10–20 s
Step 2	15%HF + 85% H ₂ O ₂	1–2 s
Step 3	1%HF + 4% H ₂ O ₂ + 20% H ₃ PO ₄ + 75% H ₂ O (distilled water)	10–20 s

growth behaviour. To obtain a sufficient number of grains, several photographs were taken which cover a relatively large number of grains at sufficient resolution of etch-pit figures. Etch-pits and grain boundaries were digitized using an image analyser. The data collected in this way was used in a program that calculates grain orientation and also various other distribution functions. Three basic etch-pit shapes were considered: a square, a rectangle and a triangle. Any etch-pit shape not belonging to one of these categories was extrapolated to a triangle form.

The orientation of each grain was then described in the specimen reference frame using the Euler angles φ_1 , Φ , φ_2 (Bunge's notation [11]). Using this notation to calculate the orientation of the grains with square-shaped etch-pits, only φ_2 (or φ_1 , or the sum of φ_1 and φ_2) needs to be calculated, and this angle is measured between the edges of the square and the specimen rolling direction (RD).

In the case of rectangular etch-pits, the Euler angle φ_1 is simply defined as the angle between the RD and a side of the etch-pit defined by length l (see Fig. 1a), and φ_2 is always zero. The length of a and b have to be measured accordingly. There is, however, a unique problem associated with the calculation of the Euler angle Φ . Depending on the speed of etching, etch-pits can be partly hidden under the specimen surface when looking down at them along the specimen normal. Because of this, etch-pits that have a proper rectangular shape can be observed, or a rectangular shape that

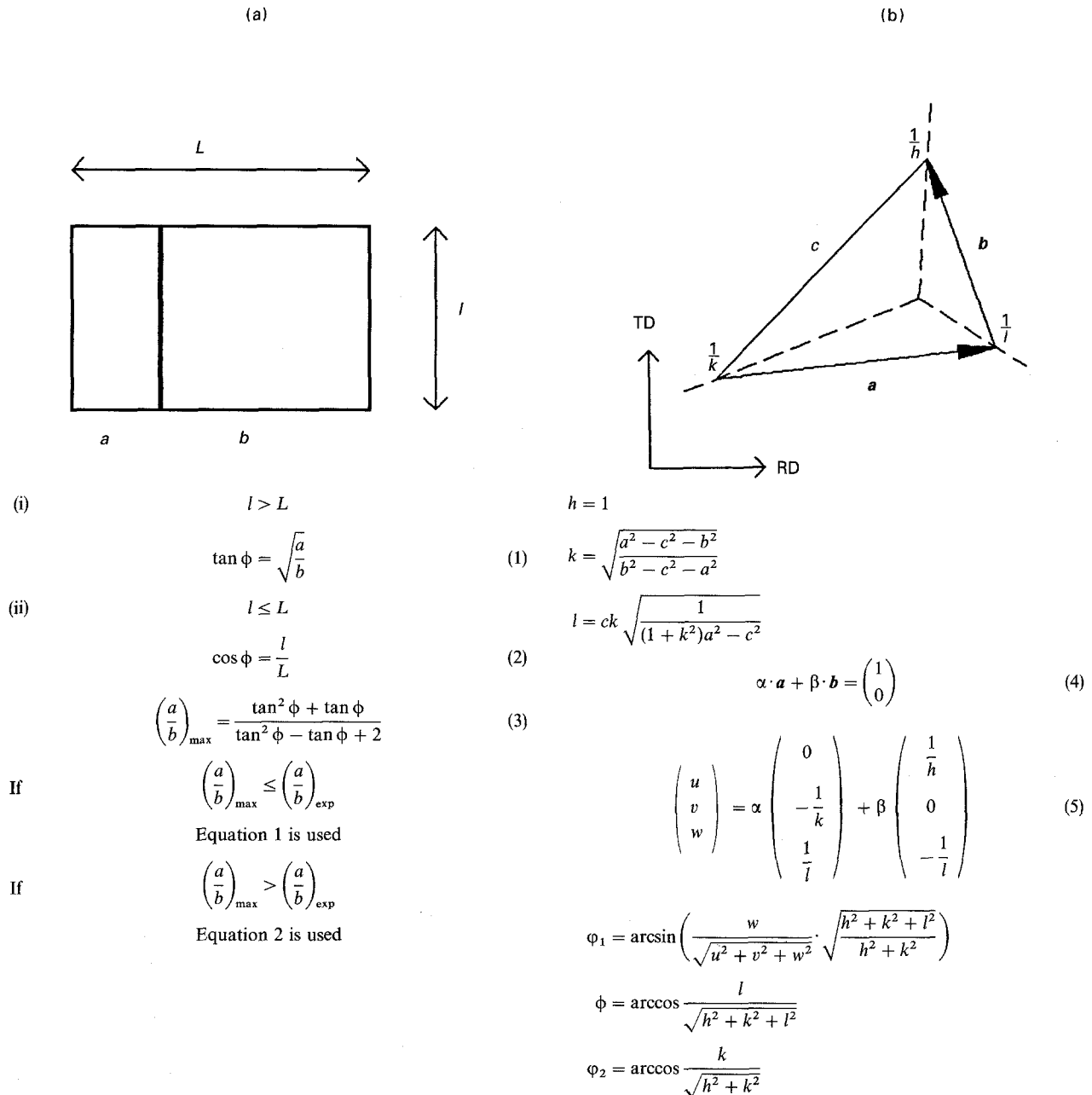


Figure 1 The Euler angles calculation of grains with (a) rectangular shape; (b) triangular shape.

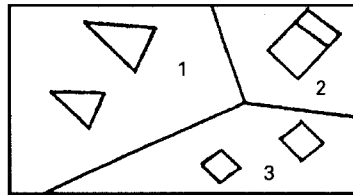
has a hidden edge. The equations used in calculating the Euler angle Φ of grains with rectangular etch-pits are summarized in Fig. 1a. In the case where there is no hidden edge ($l > L$), Equation 1 is used to calculate Φ . If there is a hidden edge ($l \leq L$), an initial estimate for Φ is calculated using Equation 2. Then, from Equation 3, the maximum possible (a/b) ratio for this estimate of angle Φ is calculated. If this maximum is smaller than the experimental (a/b) ratio, Equation 1 is used to calculate Φ . Otherwise, Equation 2 is used.

The calculation of the orientation of grains with triangular etch-pits is well described [4, 5]. In our program, formulas involving the lengths of the sides of the triangle were used instead of the cosines of the angles of the triangle. These formulas are presented in Fig. 1b, where the Miller indices, hkl , represent the orientation of the normal direction (ND) in the crystal reference frame. To obtain the grain orientation in terms of the Euler angles the coordinates uvw , representing the RD in the crystal coordinate system, are

also needed. To get these coordinates, two parameters α and β are calculated using Equation 4. Two known vectors defined in the specimen reference frame (vectors a and b in Fig. 1b) are multiplied by α and β so that the sum of the two modified vectors is parallel to the RD. The two vectors should also be known in the crystal reference frame, so that the RD can be expressed in this reference frame to form the desired uvw as given in Equation 5. Then Euler angles are calculated from the Miller indices $(hkl) [uvw]$.

Fig. 2 gives an example of the Euler angle calculation from the digitized etch-pits and grain boundaries. The standard deviation of the Euler angles and the size of each grain are also calculated.

Errors in grain orientation measurements have to be minimized to obtain a sufficient accuracy of ODF and grain misorientation analysis. Most errors that occur are caused by imperfections in the sample polishing and etching. These types of imperfections result in unclear edges on the photographs which then



gn. no.	et. no.	<i>h</i>	<i>k</i>	<i>l</i>	fil	fi	fi2
1	1	1.000	1.633	1.602	46.5	50.08	31.48
1	2	1.000	1.885	1.731	45.24	50.95	27.95
2	1	0.0000	1.000	0.8067	138.69	51.11	0.00
3	1	0.0000	0.0000	1.000	33.66	0.00	0.00
3	2	0.0000	0.0000	1.000	47.18	0.00	0.00

gr. no.	area (sqcm)*	area (%)	fil (deg)	sd. fil (rmsq)	fi (deg)	sd. fi (rmsq)	fi2 (deg)	sd. fi2 (rmsq)
1	9.3	51.79	45.69	0.5	50.52	0.4	29.71	1.8
2	3.6	20.28	138.69	0.0	51.11	0.0	0.00	0.0
3	5.0	27.94	40.42	6.8	0.00	0.0	0.00	0.0

Figure 2 Example of the screen output of the Euler angles calculated by the computer.

lead to errors in digitizing the etch-pit boundaries. Assuming that these errors are statistical errors, a standard deviation can be calculated for the Euler angles of all the etch-pits in one grain.

Fig. 3 illustrates the sensitivity of the calculated Euler angles to errors in the digitization of the corners of variously shaped etch-pits. The figure was made by creating etch-pits with the same original area and applying the same error to one corner of each of them (represented by the circle). The maximum square root of the sum of the squares of the errors in the Euler angles has been taken as a measure of the sensitivity of the calculation to the errors in the shape of the etch-pits. It is clear that the magnitude of the errors in the Euler angles depends on the shape of the etch-pits. In general, it can be concluded that square-shaped etch-pits have the smallest errors and that triangle-shaped etch-pits have the largest.

This variation in error can be explained by recognizing that square- and rectangular-shaped etch-pits have 2 and 1 Euler angles, respectively, which are predetermined. The results obtained for these kinds of etch-pits are also better because the Euler angles can be averaged 4 or 2 times because of symmetry. The errors for triangle-shaped etch-pits may seem large, but this error is calculated as the most unfavourable error. Also, the error will be reduced by averaging the angles for the number of etch-pits in each grain.

A specimen with 2 to 4 etch-pits inside each of 150 grains was analysed. The averages of the standard deviations of the Euler angles, ϕ_1 , Φ , and ϕ_2 , were 1.5, 2.9 and 2.1 deg, respectively. The experiment also showed that the errors for elongated triangular etch-pits are the largest. Special care has to be taken when extrapolating a near rectangular-shaped etch-pit into an elongated triangle.

It is possible to calculate the series expansion coefficients of the orientation distribution function directly using relations given by Bunge [11]. There is an alternative method, however, based on the assumption

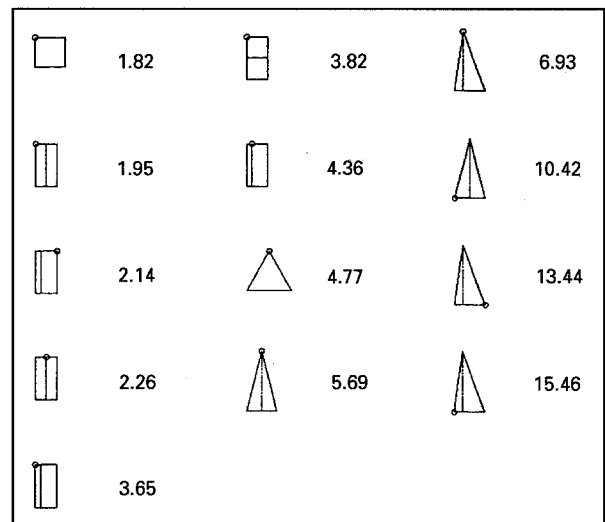


Figure 3 Shapes of the etch-pits with its maximum $(\Delta\phi_1^2 + \Delta\Phi^2 + \Delta\phi_2^2)^{1/2}$.

that Gaussian-shaped components in the orientation space correspond to the orientation of each grain. The normalized superposition of these components produces the desired texture function. This method was used to determine the ODF from the etch-pit data.

Identifying the orientation of each grain makes it possible to relate the orientations of neighbouring grains and thus calculate their misorientation. The misorientation angle is defined as the smallest of the angles corresponding to all equivalent rotations. Its distribution is well known for a randomly textured material having no correlations between grain orientations and has been obtained theoretically by Mackenzie [12] and Handscomb [13]; it is a standard distribution to which other results can be compared.

The frequency of occurrence of CSL boundaries is calculated by checking whether any of the rotations representing the misorientation of neighbouring grains coincides with the rotation corresponding to a given sigma-relationship. This procedure is repeated

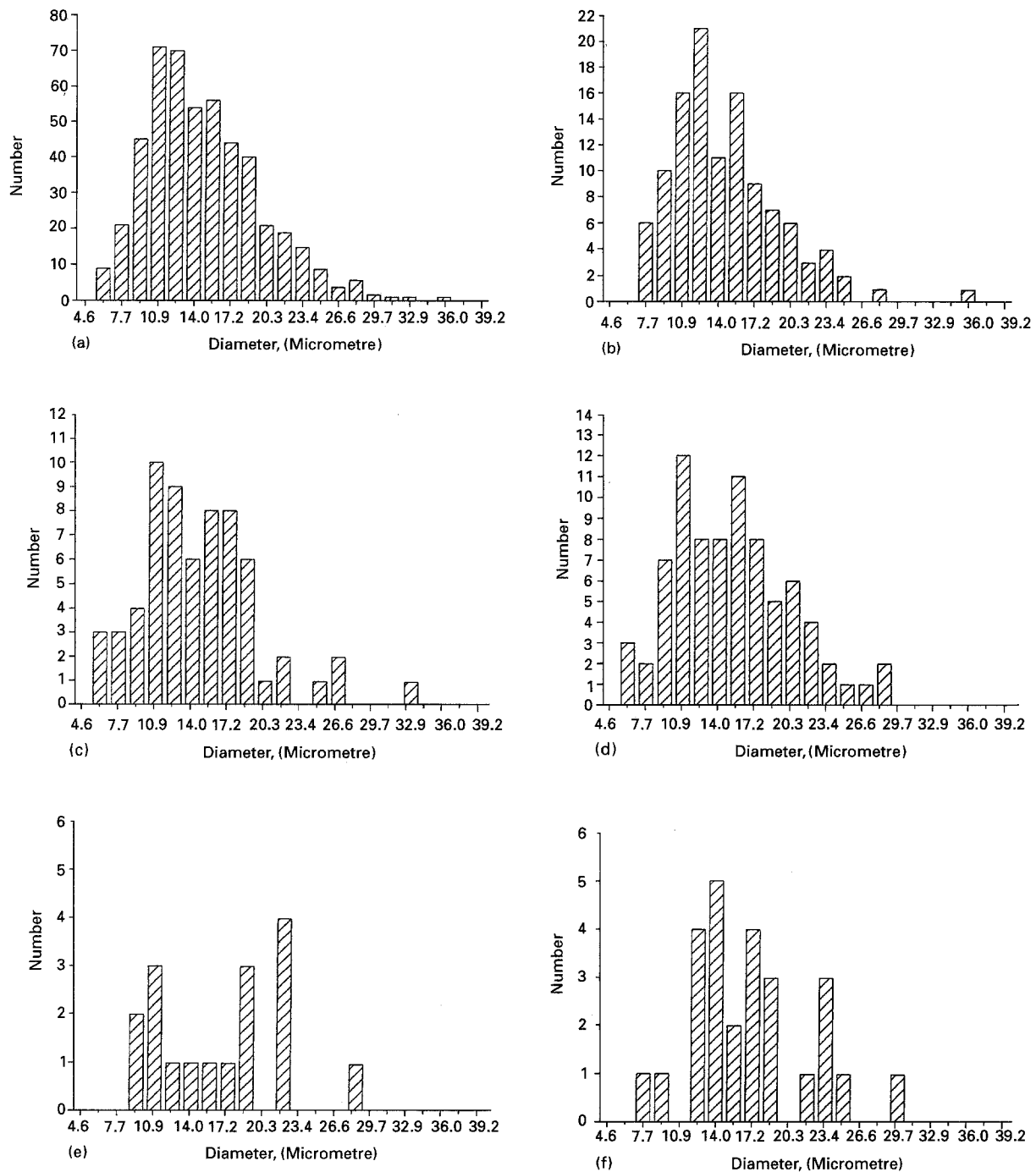


Figure 4 Grain size distribution of matrix grains and major texture components. (a) matrix grains; $\bar{D} = 14.9 \mu\text{m}$ (b) $\{111\}\langle 112\rangle$ grains; $\bar{D} = 14.7 \mu\text{m}$, vol (%) = 22.2 (c) $\{111\}\langle 110\rangle$ grains; $\bar{D} = 14.6 \mu\text{m}$, vol (%) = 12.4 (d) $\{100\}\langle 001\rangle$ grains; $\bar{D} = 15.1 \mu\text{m}$, vol (%) = 17.1 (e) $\{100\}\langle 011\rangle$ grains; $\bar{D} = 16.6 \mu\text{m}$, vol (%) = 4.9 (f) $\{110\}\langle 001\rangle$ grains; $\bar{D} = 17.0 \mu\text{m}$, vol (%) = 7.9.

for every sigma-relationship up to $\Sigma 51$ and for every pair of neighbouring grains. Coincidence is defined by the Brandon criterion [14] (the rotations are considered to coincide if the misorientation angle between them is smaller than $15^\circ/\sqrt{\Sigma}$). To account for different surface areas of the grain boundaries, it was assumed that the area of the smaller grain is a good measure of the grain boundary area.

3. Results

An Fe-3%Si sheet was used to illustrate the etch-pit method for texture analysis. Fig. 4 shows the grain size distribution of all grains obtained from the etch-pit

analysis, as well as the major texture components such as the $\{111\}\langle 112\rangle$, $\{111\}\langle 110\rangle$, $\{100\}\langle 001\rangle$, $\{100\}\langle 011\rangle$ and the $\{110\}\langle 001\rangle$. About 500 grains were analysed for this study. As shown in Fig 4, the $\{111\}\langle 112\rangle$, texture component accounted for 22% of the matrix volume, while Goss grains accounted for only 8%. The average diameter of the Goss grains was $17 \mu\text{m}$ which is bigger than any other grains.

Fig. 5 shows the orientation distribution function (ODF) calculated from both the etch-pit and standard X-ray diffraction methods. There appears to be a qualitative agreement between these ODFs. A certain discrepancy exists between the ODFs for those

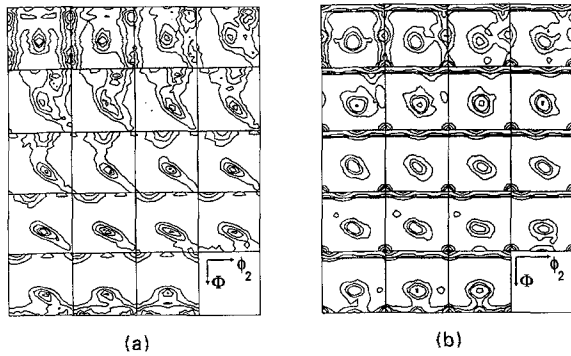


Figure 5 Orientation distribution function (ODF) obtained from (a) X-ray diffraction method; (b) etch-pit method.

orientations where $\langle 100 \rangle$ is parallel to rolling direction.

To help understand grain growth behaviour, the grain boundary character between a growing grain and matrix grains has been studied [15, 16]. It is believed that the difference in mobility of special grain boundaries is responsible for the texture development; however, the method used for these studies was time consuming and complicated. One of the advantages of

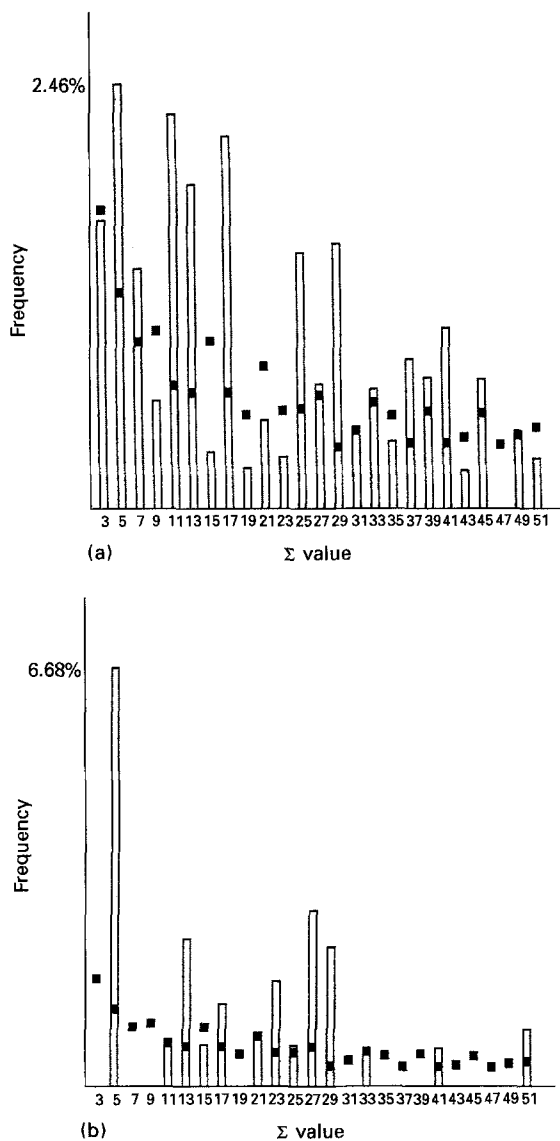


Figure 6 Distribution of CSL boundaries of (a) matrix grains; (b) Goss grains.

the etch-pit technique is that one can easily get information about the coincidence site lattice relationships (misorientation relationship) between neighbouring grains. The best known statistical characteristics of misorientation are the distribution of the misorientation angles and the frequency of occurrence of low-sigma CSL boundaries which exert beneficial effect on various properties of polycrystalline materials. The histogram of the CSL boundary distribution up to $\Sigma 51$ from all grains is shown in Fig. 6a, and another histogram describing the misorientation between grains having $\{110\}\langle 001 \rangle$ orientation and neighbouring grains is given in Fig. 6b. The black squares in both CSL histograms represent the frequency of the CSL boundaries in the case of a non-textured specimen. Comparing the CSL distribution from the Goss grains to that from all grains, it is observed that the $\{110\}\langle 001 \rangle$ grains have a higher amount of $\Sigma 5$, $\Sigma 27$, and $\Sigma 29$ CSL boundaries while the CSL distribution from all grains shows a higher amount of $\Sigma 11$ and $\Sigma 25$ CSL boundaries. Fig. 7a

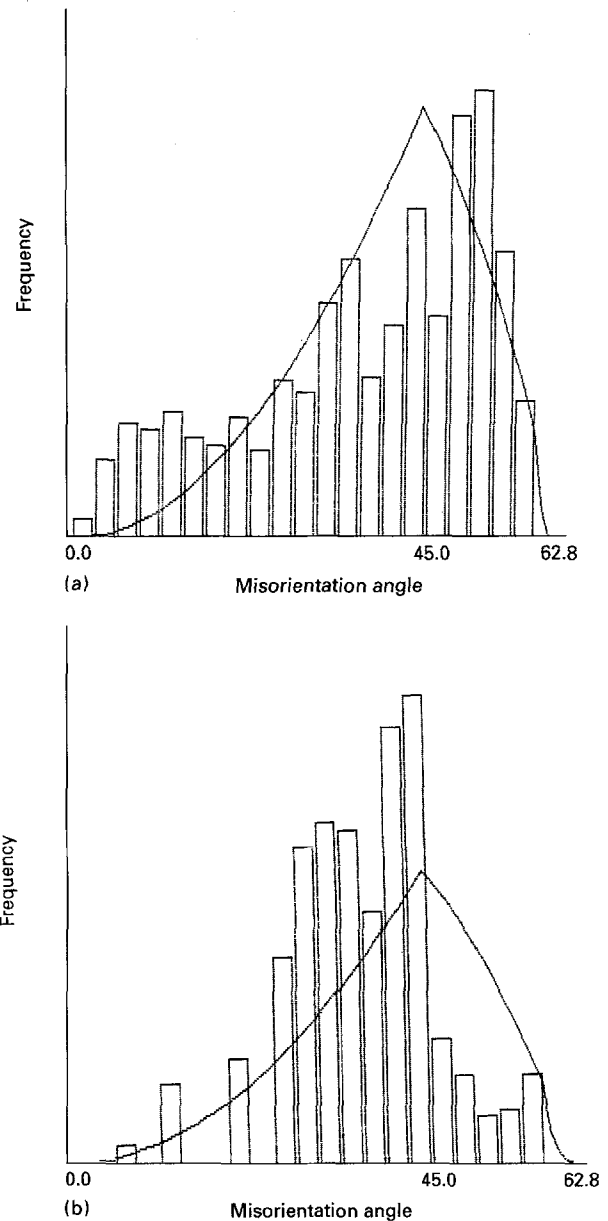


Figure 7 Misorientation angle distribution of (a) matrix grains; (b) Goss grains.

shows the distribution of the misorientation angle from the grains, and Fig. 7b shows that from the Goss grains and neighbouring grains. The misorientation angle distribution for a non-textured specimen is shown as the curved line. It can be seen that the matrix grains have a larger amount of less mobile, low angle (less than 20°) misorientation boundaries.

The etch-pit method can be used in a number of different research areas, for instance in research on texture development during secondary recrystallization or the study of intergranular stress corrosion cracking [17].

4. Conclusion

The etch-pit technique can be used for a quantitative texture analysis and description of polycrystalline materials. Etch-pit experimental data from a Fe-3%Si steel sheet was used to obtain the crystal orientation distribution function (ODF) and the grain misorientation distribution. A computer program was developed which identifies the CSL boundaries and which can be used to obtain the frequency of CSL boundaries with respect to all matrix grains and grains having a specific orientation. In addition, grain size distributions were obtained for matrix grains and grains having a specific orientation. The etch-pit method can be applied to a number of different research areas.

References

1. L. ILLGEN, *Pract. Metallogr.* **6** (1969) 363.
2. LUO YANG, *Acta Metall. Sin.* **13** (1977) 93.
3. C. BARRETT, "Structure of Metals", (McGraw-Hill, New York, 1966).
4. ÉVA TASSY-BETZ and J. PROHÁSZKA, *Metallography* **7** (1974) 91.
5. G. E. G. TUCKER and P. C. MURPHY, *J. Inst. Met.* **8** (1952) 235.
6. LUO YANG, WANG ZHEN-CHIN and LI WEN-CHEN, *Prakt. Met.* **20** (1983) 194–200, 232–44.
7. LUO YANG and LÜ QICHUN, *Acta Metall. Sin.* **15** (1979) 235.
8. A. BÖTTCHER, T. GERBER and K. LÜCKE, *Mater. Sci. and Tech.* **8** (1992) 16.
9. G. ABBRUZZESE, A. CAMPOPIANO and S. FORTUNATI, *Textures and Microstructures*, Vols 14–18 (1991) 775.
10. S. FORTUNATI, G. ABBRUZZESE and P. E. DINUNZIO, *Mater. Sci. Forum*, Vols 94–96 (1992) 431.
11. H. J. BUNGE, "Texture analysis in Materials Science", (Butterworths, London, 1982).
12. J. K. MACKENZIE, *Biometrika* **45** (1958) 229.
13. D. C. HANDSCOMB, *Canad. J. Math.* **10** (1988) 85.
14. D. G. BRANDON, *Acta Metall.* **14** (1966) 1479.
15. J. HARASE and R. SHIMIZU, *Trans. JIMS.* **29** (1988) 388.
16. *Idem*, *Acta Metall.* **40** (1992) 1101.
17. G. PALUMBO, P. J. KING, K. T. AUST, U. ERB and P. C. LICHTENBERGER, *Scripta Metall.* **25** (1991) 1775.

*Received 30 September 1993
and accepted 27 July 1994*